

5-Amino-3-imino-1,2,6,7-tetracyano-3*H*-pyrrolizine: characterization of the solvent-free solid phase and interaction with ammonia and water

Vincenzo Fares,^{*a} Alberto Flamini,^{*†a} Donatella Capitani^b and Roberto Rella^c

^aIstituto di Chimica dei Materiali del CNR, Area della Ricerca di Roma, PO Box 10, 00016 Monterotondo Stazione, Roma, Italy

^bIstituto di Strutturistica Chimica del CNR, Area della Ricerca di Roma, PO Box 10, 00016 Monterotondo Stazione, Roma, Italy

^cIstituto per lo Studio di Nuovi Materiali per l'Elettronica del CNR, Via Arnesano, 73100 Lecce, Italy

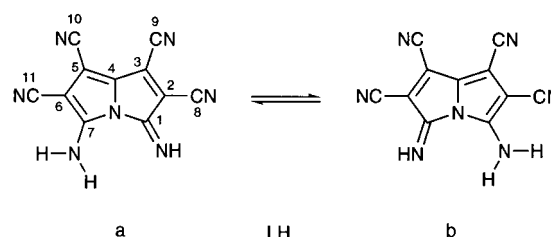
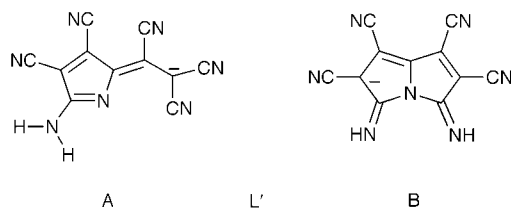
The 5-amino-3-imino-1,2,6,7-tetracyano-3*H*-pyrrolizine (LH, C₁₁H₃N₇), previously characterized as the 2:1 1-chloronaphthalene adduct, has been further investigated as a solvent-free solid phase. Strong intermolecular interactions take place in this phase, as revealed by the optical spectra of evaporated LH thin films ($\lambda_{\text{max}} = 615$ and 570 nm) compared to the optical spectrum of LH in solution ($\lambda_{\text{max}} = 580$ nm). ¹³C NMR spectra also support the occurrence of intermolecular attractive CN group interactions in the solid state. X-Ray diffraction patterns indicate that the controlled sublimation process of LH ($T_{\text{subl}} = 200$ °C, 10^{-6} mmHg) leads to films composed of highly oriented crystallites, with two main sets of diffracting planes parallel to the film surface. The refractive index of LH as an evaporated thin film has also been determined in the 400–800 nm spectral range ($n = 1-2$). LH interacts with ammonia and/or water in the gas phase. In the first case the acid–base reaction ($\text{LH} + \text{NH}_3 \rightleftharpoons \text{L}'\cdot\text{NH}_4^+$) occurs. The resulting L' anion ($\text{L}' = \text{C}_{11}\text{H}_2\text{N}_7^-$) is the 2-(5-amino-3,4-dicyano-2*H*-pyrrol-2-ylidene)-1,1,2-tricyanoethanide (**A**, $\lambda_{\text{max}} = 525$ nm) or the isomer 1,2,6,7-tetracyano-3,5-dihydro-3,5-diiminopyrrolizinide (**B**, $\lambda_{\text{max}} = 680$ nm), depending on the relative amount of water to ammonia in the gas phase. This reaction is driven by the hydrogen bonding of NH_4^+ to **B** and/or to water. In the second case a fast proton scrambling occurs.

We have recently synthesized and structurally characterized the title pyrrolizine (LH, Scheme 1) as the 2:1 1-chloronaphthalene adduct: 2LH·NAPH.¹ Our interest in LH is mainly due to its chemico-physical properties: (i) it is a planar, intensely coloured molecule [in tetrahydrofuran (THF): $\lambda_{\text{max}} = 580$ nm, $\epsilon_{580} = 20\,000$ dm³ mol⁻¹ cm⁻¹], (ii) it can develop attractive potentials in the solid state through several mechanisms such as π -orbital overlap, hydrogen bonding, dipolar CN group interactions, (iii) it forms mono- and/or bis-pyrrolizinato metal complexes, (iv) it can be deposited under vacuum as thin films and (v) in this state it is a semiconductor of low conductivity. In research aimed at addressing its possible use in technological applications, by analogy with molecular materials based on evaporated dyes and/or semiconductors,² LH has been further characterized both in solution and in the solid state. Moreover, we investigated whether LH has any recognition properties for selective detection of species of environmental interest in air. Herein the results of these studies are reported.

Experimental

Materials

LH was prepared from NaL' according to the previously reported procedure.¹



Scheme 1 Non-systematic numbering is used for the NMR assignments

It was recrystallized from acetone–water (1:1) and then dried in an oven at 60 °C in air for 4 h. From thermal gravimetric and differential analyses, performed with a Du Pont 950 apparatus, it did not show any weight loss nor heat exchange up to 250 °C. Its density (d) was measured (1.45 g cm⁻³) by suspending the powder in a suitable mixture of solvents. Evaporated films were deposited on glass plates in an Edwards Auto 306 vacuum coater as described previously.¹ LH can be fully deuterated on exposure to D₂O vapor in a dry-box, as proved by the infrared spectra (Fig. 11; see later). Spin coated films were deposited from a THF solution with a Convac spinner model 1001. Film thicknesses were measured using an Alpha-Step stylus profilometer. Scanning electron microscopy (SEM) images were recorded on a JEOL SM6100 instrument.

Powder X-ray diffraction (XRPD)

X-Ray diffraction data, both for powder samples and for polycrystalline thin films, were collected on a Seifert XRD3000 two-circle automated diffractometer at room temperature using Cu-K α radiation with a graphite monochromator. The step scanning technique, with steps of $2\theta = 0.025^\circ$ and a stepping time of 10 s, was used over the range $5^\circ \leq 2\theta \leq 50^\circ$.

† E-mail: flamini@nserv.icmat.mlib.cnr.it

Optical and infrared spectroscopic measurements

Optical spectra were recorded on a Cary 5 spectrometer. Dried and freshly distilled solvents were used for the solution spectra. The spectra of the films were measured by inserting the glass slide supporting the film vertically across the light beam into a 10 mm square quartz cuvette. An uncoated glass slide was placed in the reference compartment. In addition, reflectivity measurements in the 400–800 nm spectral range were carried out using the integrating sphere accessory of the spectrophotometer.

IR spectra were recorded on a Perkin Elmer 16F PC FT-IR spectrometer as Nujol mulls.

¹³C NMR measurements

Solid state ¹³C CP-MAS NMR spectra at 50.13 MHz were recorded on a Bruker AC-200 spectrometer, equipped with an HP amplifier, 1 H 200 MHz, 120 W cw, and with a pulse amplifier, M3205. The spin rate of the sample was 8 kHz. The $\pi/2$ pulse width was 3.1 μ s, the contact time for the cross-polarization experiment was 4 ms and the relaxation delay was 10 s. ¹³C spectra were obtained with 512 words in the time domain, zero filled and Fourier transformed with a size of 1 K.

All the solution experiments were performed on a Bruker AMX-600 spectrometer. High resolution ¹³C NMR spectra at 50.9 MHz were obtained with broad band proton decoupling performed with a GARP sequence.³ Acquisition and relaxation delay were chosen according to the Ernst relationship⁴ in order to maximize the signal to noise ratio for the long relaxation of quaternary C atoms. Spectra were obtained with 16 K words in the time domain and Fourier transformed on a size of 8 K.

Electrical resistivity measurements and sensor property studies

Electrical measurements were performed on our samples in order to test the electrical sensing properties of the active layer. To this end, alumina substrates were first prepared by thermal evaporation and deposition of a patterned microelectrode array consisting of interdigitated pairs of gold fingers about 40 nm thick. The dc resistance of the various samples was measured by an electrometer, Keithley model 617. The average resistivity of the samples of typical dimension $1 \times 1 \times 1.5 \times 10^{-5}$ cm³ measured in a flux of dry air was about 1.7×10^6 Ω cm. The effect of different toxic gases on electrical conductivity was measured in a dynamic pressure system implemented in our laboratory where dry air at ambient pressure was used as the carrier and reference gas. The gas concentration was varied by using a MKS Instrument mass flow controller, model 647.

Results and Discussion

For our objectives, one of the most relevant properties of LH is that it sublimates without decomposition affording thickness-controlled thin films. Thus, the following discussion deals mainly with different sets of experimental data for LH in the solvent-free solid phase, either as a powder or thin films. When appropriate, a comparison with the corresponding data for 2LH·NAPH and of LH in solution is made.

X-Ray diffraction patterns

XRD measurements were made on several samples. (i) Solvent-free microcrystalline powder was obtained as described in the Experimental. The corresponding XRPD pattern [Fig. 1(b)] shows a series of broad peaks characterized by FWHM values in the range 0.30–1.20°; this indicates a poorly crystalline structure. Consequently, any attempt to indicize the spectrum failed. The main peaks (interplanar distances, in Å) and their relative intensities (in parentheses), are as follows: 9.04(9), 8.26(39), 5.57(61), 5.21(28), 4.54(21), 4.02(21), 3.50(8),

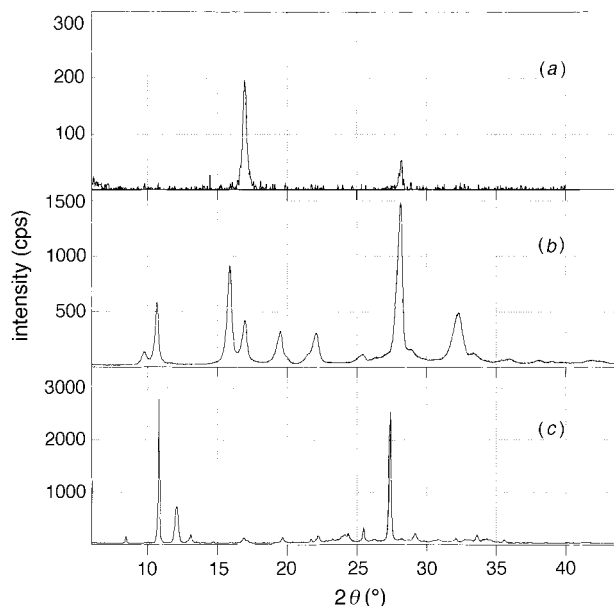


Fig. 1 XRD patterns of different samples of LH: (a) evaporated film, (b) solvent-free microcrystalline powder and (c) microcrystalline 2LH·NAPH

3.17(100), 2.76(32). (ii) Microcrystalline 2LH·NAPH, of known structure.¹ From the corresponding XRPD [Fig. 1(c)] it shows a much higher degree of crystallinity in this case, the FWHM ranging from 0.12 to 0.90°. (iii) Microcrystalline powder, obtained by accurate grinding of LH evaporated films. Its diffraction pattern is identical with that of powder (i), so proving that the films deposited by sublimation have the same crystal structure as the source powder. (iv) LH deposited under vacuum as thin films. Several samples of different thickness (50–800 nm) have been examined. Their XRD patterns are all identical: the one relating to a 400 nm thin film is reported in [Fig. 1(a)]. As only two peaks are present, at 5.21 and 3.17 Å, replacing the set of peaks from the same films once ground (see point iii), we must infer that the controlled sublimation process leads to thin films constituted of highly oriented crystallites, with two main sets of diffracting planes parallel to the film surface, with interplanar distances typical for face-to-face π -interacting conjugated systems, so suggesting a deposition process leading to face-to-face LH units.

Optical spectra

Evaporated thin films deposited on glass showed well resolved optical spectra. From these spectra, after normalization to the concentration of LH in the solvent-free solid phase ($C = 6.2$ M) and to the film thickness, the molar extinction coefficient (ϵ) of LH in the film *vs.* wavelength can be calculated. On comparison with the corresponding values of LH in solution (Fig. 2) a remarkable feature appears. The single band of LH in solution ($\lambda_{\text{max}} = 580$ nm) is replaced in the solid state by a double band ($\lambda_{\text{max}} = 615$ and 570 nm) of approximately the same total area and with two associated components of the same intensity. Clearly, such spectral variations originate in solid-state intermolecular interactions. In this regard, either of the following mechanisms could be in operation, depending on the crystal structure: the well-known Davydov-type coupling⁵ or a charge-transfer between adjacent molecules, which occurs widely in polycyano-substituted molecules.⁶ Occasionally, some evaporated thin films, as well as the spin-coated films, showed optical spectra quite different from that just discussed. In Fig. 3 the spectra in question, derived from evaporated LH films of the same thickness, are reported: spectrum 1 exhibits more than the two bands expected for exciton splitting within the crystal as usually observed (spec-

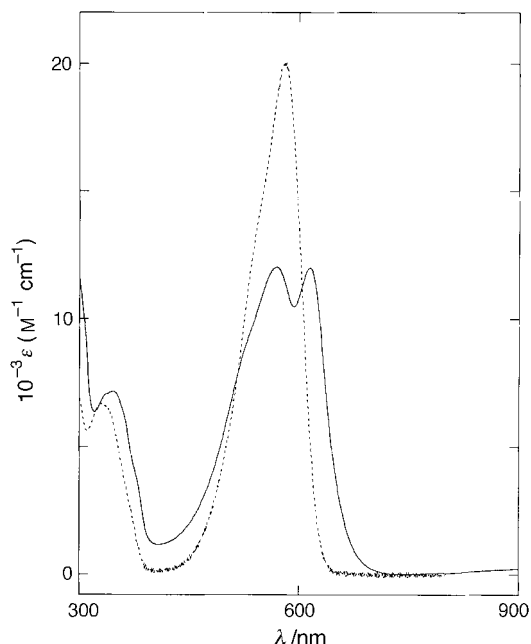


Fig. 2 Normalized optical spectra of LH: (—) as evaporated film and (----) in THF solution

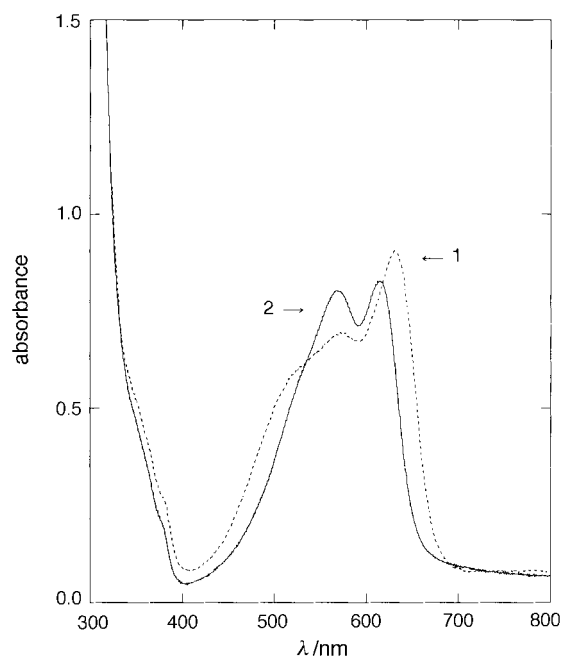


Fig. 3 Optical spectra of two different LH evaporated films of the same thickness (150 nm)

trum 2). In conjunction with the SEM images of the source films (1' and 2' of Fig. 4), this could be explained by the different film morphology, which may imply a larger amorphous content in 1', than in 2'. In turn, 2' clearly shows a layered crust probably of crystalline structure.

The refractive index n of the as-deposited LH thin films *vs.* wavelength was also calculated from a computer fit of both transmission $T(\lambda)$ and reflection $R(\lambda)$ measurements based on a model that considers a parallel sided isotropic and absorbing film between transparent media of indexes n_0 (air) and n_2 (glass substrate), the latter being assumed to be very thick with respect to the wavelength.⁷ Fig. 5 shows the refractive index n of a typical evaporated LH thin film in the 400–800 nm spectral range. As can be seen, the refractive index n of the film changes slowly between 1 and 2.

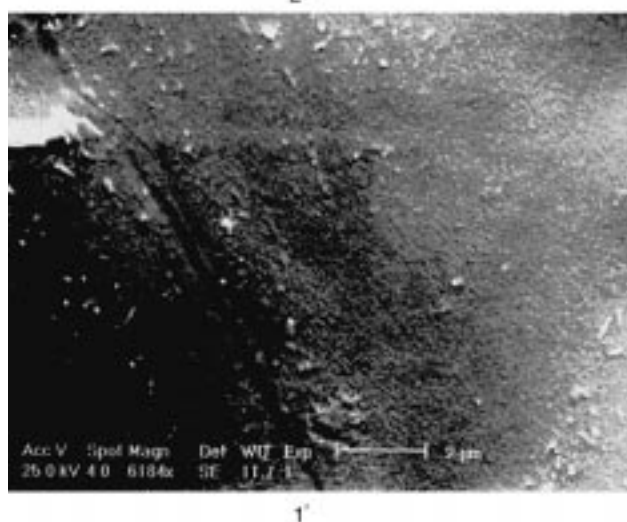


Fig. 4 SEM micrographs of the LH evaporated films, whose optical spectra are reported in Fig. 3

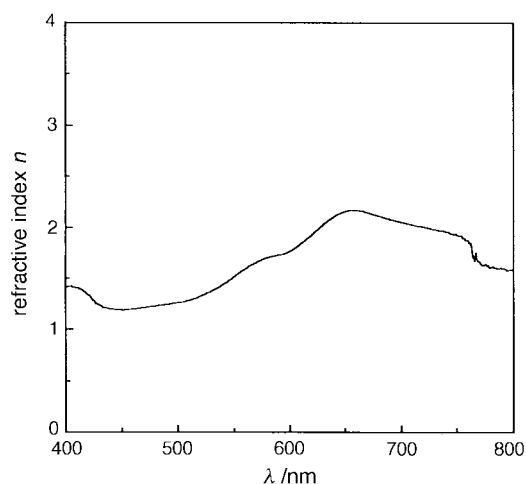


Fig. 5 Refractive index (n) *vs.* wavelength for a typical evaporated LH thin film

¹³C NMR spectra

Before examining these data, let us consider the tautomerism between the two energetically equivalent LH configurations (a and b in Scheme 1), which would directly influence the NMR spectra. Previously we ascertained that such tautomerism exists only in solution. Accordingly, it was found that the N–H proton exchange at room temperature is fast in THF solution

as revealed by the ^{13}C NMR spectrum of LH in this solvent, while it does not occur in the solid state for the 1-chloronaphthalene adduct, as proved by the successful refinement of the molecular structure of LH from the single crystal X-ray analysis of $2\text{LH}\cdot\text{NAPH}$. These findings indicate that the tautomerism in question requires an intermolecular exchange mechanism. The current ^{13}C NMR data, as it will be seen, substantiate the supposed mechanism and in addition indicate that the N—H proton exchange even in solution can be slowed down by a suitable solvent such as dimethoxyethane (DME). Thus, LH in DME exhibits eleven ^{13}C NMR resonances (Fig. 6). The assignments, presented in Table 1, are based on the correlation between the observed intensity of the resonance with the relaxation time of the carbon atom originating from the resonance itself.⁸ That is, the nearer the carbon atom is to an efficient relaxation center, *i.e.* a proton, the higher the intensity of the associated resonance. The NMR spectrum of the solid shows a clear correspondence with the solution spectrum, for the most intense peaks. Two extra broad resonances appear in the solid spectrum, absent in the solution spectrum, at limiting high field (110 ppm). We tentatively assigned these resonances to the nitrile carbon atoms, whose resonance is broadened by the ^{14}N quadrupole, which in turn is averaged

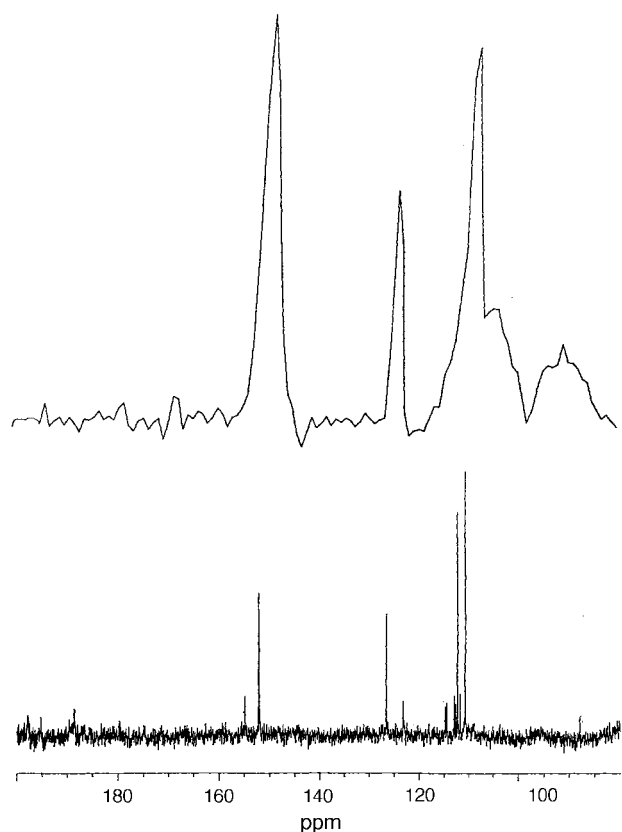


Fig. 6 ^{13}C NMR spectra of LH as solid sample (top) and in DME solution (bottom)

Table 1 ^{13}C solution and CP-MAS NMR spectral data of LH^a

Assignment ^b	δ		Assignment ^b
	Solution	Solid	
C ¹ , C ⁷	110.8, 112.35	110	C ¹ , C ⁷ , C ³
C ² , C ⁶	126.6, 152.15	107, 92	C ⁸ , C ⁹ , C ¹⁰ , C ¹¹
C ⁸ , C ⁹ , C ¹⁰ , C ¹¹	114.8, 114.5, 113.1, 112.7		
C ³ , C ⁵	111.8, 123.2	125	C ² , C ⁵
C ⁴	154.9	150	C ⁴ , C ⁶

^aSee Experimental for details of data collection. ^bSee Scheme 1 for the numbering.

to zero in solution. The resonances of these carbons are shifted to high field either due to intermolecular attractive CN group interactions⁹ or by the magnetic anisotropy of a neighboring CN group.¹⁰

Sensing properties of LH

In view of the utilization of LH for detecting species of environmental interest in the air, we probed LH films, deposited on interdigitated electrodes, as conductimetric sensors. No significant variations in their electrical conductivity were observed on exposure to NH_3 , NO , CO or H_2 gas up to 100 ppm in dinitrogen. However, see the following section.

Interaction with ammonia

The interaction of LH with NH_3 occurs only in the presence of water and it depends markedly on the experimental conditions. We selected and present here three typical examples. (1) When NH_3 (500 ppm in N_2) is slightly humidified, by passing over liquid water before interacting with LH, the spectral changes occurring (Fig. 7) are not fully reversible and, on comparison with the results of the subsequent experiments (2 and 3), they indicate the formation of two species in the film, **A** and **B** ($\lambda_{\text{max}} = 525$ and 680 nm, respectively). (2) Only **B** is formed when experiment (1) is carried out immediately after exposing the film to a water-free ammonia stream. In this case, the film will sense a smaller amount of water relative to the ammonia content in the gas phase. The consequent modification occurring is rapid and irreversible (Fig. 8). In (3), only **A** is formed when LH comes into contact, in air, with the saturated vapor of a concentrated aqueous ammonia solution (35 wt%). In this case the interaction is fully reversible, so that LH is reformed from **A** in the absence of ammonia in air with an associated negligible hysteresis (Fig. 9).

On the basis of our previous studies on LH and of the well-known solvation effects on the basicity of NH_3 ,¹¹ the results of the above experiments can be reasonably interpreted as follows. **A** and **B** are simply *L'* isomers, resulting from the same reaction $\text{LH} + \text{NH}_3 \rightarrow \text{NH}_4^+ \cdot \text{L}'$. LH is a weak acid and it reacts with NH_3 provided that the resulting NH_4^+ is

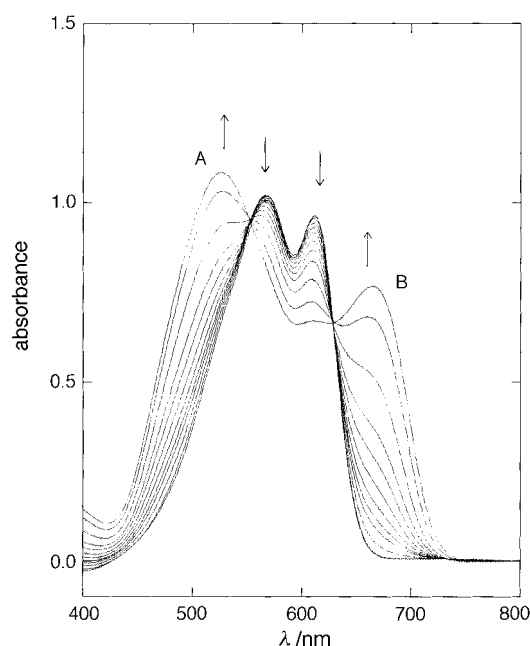


Fig. 7 Spectral changes with time (every 2 min) undergone by a thin film of LH (thickness 150 nm) on exposure to NH_3 (500 ppm in N_2) humidified by passing over liquid water. The arrows indicate the direction of the spectral changes.

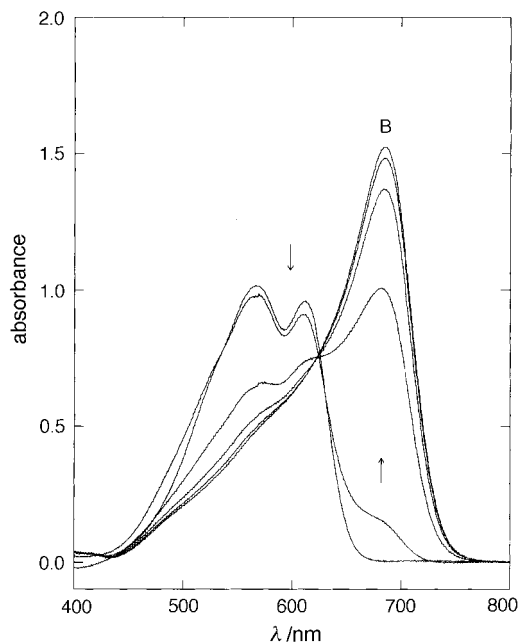


Fig. 8 Spectral changes with time (every 1 min) undergone by a thin film of LH (thickness 150 nm) on exposure to NH_3 as described in Fig. 7. In this case, the film was previously exposed to a water-free ammonia stream immediately before the interaction with humidified ammonia (see text). The arrows indicate the direction of the spectral changes.

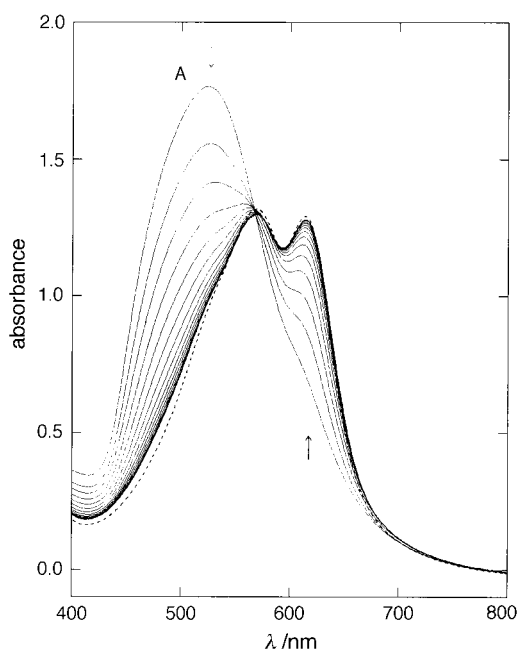


Fig. 9 Spectral changes with time (every 20 min) undergone by a thin film of LH (thickness 170 nm) after exposure to the saturated vapor of a concentrated aqueous ammonia solution (35 wt%). The arrows indicate the direction of the spectral changes. (---) Spectrum of the sample prior to exposition to $\text{NH}_3\text{-H}_2\text{O}$ vapor.

efficiently solvated. This may likely occur with the intervening four hydrogen bonds.

So, NH_4^+ forms four hydrogen bonds with four H_2O molecules if there is enough water available in the system then L' adopts the most stable configuration **A** as in experiment (3). Alternatively, NH_4^+ forms two hydrogen bonds with two H_2O molecules and two others with the imino groups of isomer **B** as in the experiment (2) if there is little water available. We note that in the latter case, **B** itself, which so far was known to exist only when coordinated to a late transition

metal [e.g. Zn^{II}], is stabilized by hydrogen bonding to NH_4^+ . At the end of experiment (1), NH_4^+ will be solvated partly as $\text{NH}_4^+ \cdot 4\text{H}_2\text{O}$ lying close to **A** as the counteranion and partly as $\text{B} \cdot \text{NH}_4^+ \cdot 2\text{H}_2\text{O}$. For further support of this explanation, we report (Fig. 10) the normalized solution optical spectra of $\text{AsPh}_4 \cdot \text{L}'$ and $(\text{acac})\text{ZnL}'$ ($\text{acac} = \text{acetylacetonato}$), both structurally characterized,^{12,13} as representative examples of the isomers **A** and **B**, respectively. Note that LH, due to the absence of mesomeric resonance, exhibits a less intense spectrum relative to **A** and **B** both in solution and in the solid state. Finally, as implicated by these findings, we infer that LH could be used as a specific optical sensor for ammonia in air under rigorously humidity controlled conditions. Such a sensor would be highly desirable for practical use, given that the existing ones lack selectivity as they are based on pH indicator dyes.¹⁴ In our laboratory, several trials are in progress to this end.

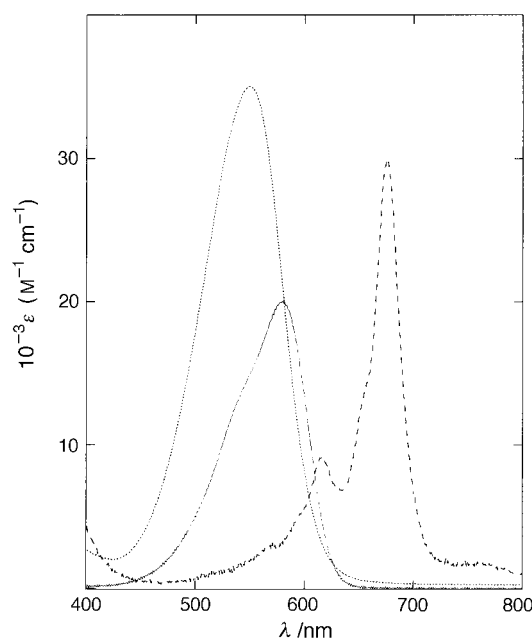


Fig. 10 Normalized solution optical spectra of (-----) $\text{AsPh}_4 \cdot \text{L}'$ in THF, (—) LH in THF and (---) $(\text{acac})\text{ZnL}'$ in toluene

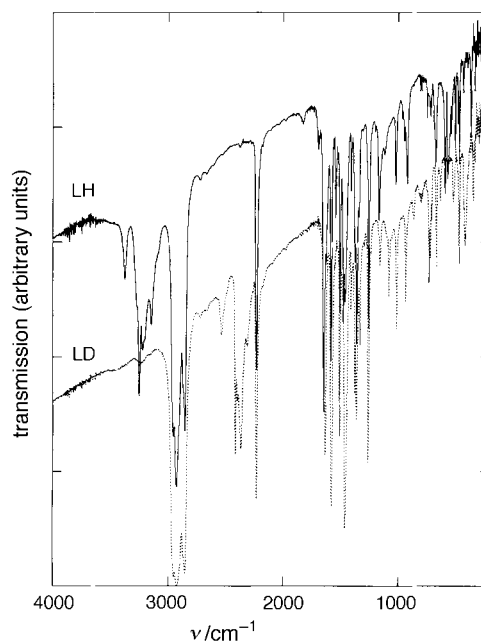


Fig. 11 Infrared transmission spectra of (—) LH and (-----) LD both as Nujol mulls

Interaction with water

LH in the solid state interacts with water vapor, causing fast and quantitative scrambling protons, despite its lack of affinity for water. This property is remarkable and in the appropriate conditions can be exploited for detecting water in air by means of infrared spectroscopy. For instance, LH can be easily fully deuterated (see Experimental). In the 3500–3000 cm^{-1} IR spectrum of the deuterated species, say LD, this region lacks any absorptions (Fig. 11). On exposure to air, the strong N–H stretching vibration infrared-active absorptions appear in this spectral region as a consequence of the transformation LD→LH by water vapor. In no case is water (H_2O or D_2O) trapped in the sample, thus avoiding the additional complication of discriminating between O–H(D) and N–H(D) absorptions in evaluating IR sensor applications. It is also found, as expected, that this transformation is chemically fully reversible.

We thank the Progetto Strategico ‘Materiali Innovativi’ of CNR for partial financial support, Mr Claudio Veroli for technical assistance during the X-ray work and Dr A. Capobianchi for help in the experiments with ammonia.

References

- 1 V. Fares, A. Flamini and N. Poli, *J. Am. Chem. Soc.*, 1995, **117**, 11 580.
- 2 H. Böttcher, T. Fritz and J. D. Wright, *J. Mater. Chem.*, 1993, **3**, 1187.

- 3 A. J. Shaka, P. B. Baker and R. Freeman, *J. Magn. Reson.* 1985, **64**, 547.
- 4 R. R. Ernst, G. Bodenhausen and A. Wokaun, *Principles of Nuclear Magnetic Resonance in One and Two Dimensions*, Clarendon Press, Oxford, 1987, ch. 4, p. 125.
- 5 M. Pope and C. E. Swenberg, *Electronic processes in organic crystals*, Oxford University Press, New York, 1982, p. 59.
- 6 (a) M. Bonamico, V. Fares, A. Flamini, A. M. Giuliani and P. Imperatori, *J. Chem. Soc., Perkin Trans. 2*, 1988, 1447; (b) M. Bonamico, V. Fares, A. Flamini and P. Imperatori, *J. Chem. Soc., Perkin Trans. 2*, 1990, 121; (c) M. Bonamico, V. Fares, A. Flamini, P. Imperatori and N. Poli, *J. Chem. Soc., Perkin Trans. 2*, 1990, 1359; (d) V. Fares, A. Flamini and N. Poli, *J. Chem. Res.*, 1995, (S) 494; (M) 3054.
- 7 O. S. Heavens in *Physics of thin Films*, ed. G. Hass and R. E. Thun, Academic Press, New York, 1964, p. 193.
- 8 E. Breitmaier and W. Voelter, *^{13}C NMR Spectroscopy*, 2nd edn., Verlag Chemie, New York, 1978, p. 111.
- 9 J. B. Stothers, *Carbon-13 NMR Spectroscopy*, Academic Press, New York, 1972, p. 226
- 10 J. A. Polple, *J. Chem. Phys.*, 1956, **24**, 1111.
- 11 F. E. Condon, *J. Am. Chem. Soc.*, 1965, **87**, 4481.
- 12 V. Fares, A. Flamini and N. Poli, *J. Chem. Res.*, 1995, (S) 228; (M) 1501.
- 13 V. Fares and A. Flamini, to be published.
- 14 (a) C. Preininger, G. J. Mohr, I. Klimant and O. S. Wolfbeis, *Anal. Chim. Acta*, 1996, **334**, 113; (b) A. Mills, L. Wild and Q. Chang, *Mikrochim. Acta*, 1995, **121**, 225; (c) R. Klein and E. Voges, *Fresenius J. Anal. Chem.*, 1994, **349**, 394; (d) A. Sansubrinio and M. Mascini, *Biosens. Bioelectron.*, 1994, **9**, 207; (e) Y. Sadaoka, Y. Sakai and M. Yamada, *J. Mater. Chem.*, 1993, **3**, 877; (f) Y. Sadaoka, Y. Sakai and Y. Murata, *Talanta*, 1992, **39**, 1675; (g) P. Çağlar and R. Narayanaswamy, *Analyst*, 1987, **112**, 1285; (h) J. F. Giuliani, H. Wohltjen and N. L. Jarvis, *Opt. Lett.*, 1983, **8**, 54.

Paper 7/06942A; Received 25th September, 1997